25th ABCM International Congress of Mechanical Engineering
October 20-25, 2019, Uberlândia, MG, Brazil

CFD FLAMELET APLICATION OF NON-PREMIXED DIESEL TURBULENT COMBUSTION: DROPLET SIZE INFLUENCE

Raul Vanz
Paulo Rodolfo Buffon Ortiz
Paulo Smith Scheneider
Department of Mechanical Engineering – Federal University of Rio Grande do Sul – UFRGS
Sarmento Leite Street, n.° 425, Cep 90050-170, Porto Alegre, RS, Brazil
vanzraul@gmail.com, pbuffono@gmail.com, pss@mecanica.ufrgs.br

Cristiano Vitorino da Silva
Department of Engineers and Computational Science – Regional Integrated University of Alto Uruguai and Missions - URI
Sete de Setembro Avenue, n. 1621, Cep 99700-000, Erechim, RS, Brazil.
cristiano@uricer.edu.br

Guilherme Lacerda Batista de Oliveira
Energy of Portugal – EDP
CE-085 Highway, km 37.5, Cep 62670-000, São Gonçalo do Amarante, CE, Brazil.
guilherme.oliveira@edpenergiapecem.com.br, tarcisio.pimentel@edpenergiapecem.com.br

Abstract.
This work presents a tridimensional numerical simulation of the non-premixed combustion of diesel in atmospheric air, inside a circular combustion chamber, used for ignition of the Doosan Babcock Mark III low-NOx burner type AASB, in order to adequacy of the application of the laminar flamelet concept on the numerical simulation of multidimensional non-premixed diesel flames, as well as to verify the behavior of the flow in front of the imposed boundary conditions. The simulation is based on the solution of mass, energy, momentum and chemical species conservation equations. Thermal radiation exchanges in the combustion chamber are computed through the Discrete Transfer Radiation Model (DTRM), and the gas absorption coefficient dependence on the wavelength is predicted by gray gas model. The turbulence is modeled by the standard $k-\varepsilon$ model, and the chemical reactions by a PDF-flamelet model. The finite volume method is employed to treat the differential equations by using the commercial software Ansys CFX in the simulations. Two cases were considered with different droplet sizes, 90 μm and 50 μm. Results indicate that the flame is relatively short as expected. It was observed that large drops need more energy to evaporate, consequently removing energy from the flame and lowering the temperature of the flame. In addition, it was also observed that smaller droplets tend to have a more intense flame region, having their evaporation and oxidation closer to the fuel injection region.

Keywords: *Flamelet, Diesel Combustion, CFD, Representative Interactive Flamelet, Droplet Evaporation.*

1. INTRODUCTION

Fluid dynamics, heat and mass transfer phenomena involved in combustion systems is governed by continuity, momentum, energy and species transport equations, as well as other constitutive equations as state equation, reaction models, among others. The considerable complex phenomena involved, often three-dimensional turbulent flames with radiatively participating media and large kinetic mechanisms, hardly allow the resolution of detailed models forcing the assumption of restrictive hypothesis in the development of computational capable models.

The physical and chemical complexity of Diesel-fuel considering its many compounds imposes insurmountable problems to the diesel combustion modeling. As a solution reference fuels are considered, for which chemical reaction mechanisms have been developed, in this article pure n-decane.

Several comprehensive numerical codes have been developed to simulate Diesel-fuel oil combustion. Those codes have their unique capabilities and different levels of success when being applied to a utility boiler firing oil. All those codes assume a known droplet spray pattern, either through oil spray characterization measurements or through estimations. Droplet heat up and vaporization, gas phase combustion, soot radiation, cenosphere formation and destruction arc handled differently for different comprehensive numerical codes.

In this work, simulations were performed applying the Representative Interactive Flamelet (RIF) model is rigorously derived from the equations governing the physics of combustion and does therefore not require the tuning of parameters. Since it is based on the flamelet approach, it allows the application of detailed chemistry. Hence, auto-ignition, partially premixed burning, diffusive combustion and pollutant formation need not to be modeled separately, but are part of the

comprehensive chemical mechanism, which consists of 120 species and 883 elementary reactions including fuel oxidation, and low temperature degenerate chain branching to describe auto-ignition. The objective of this work was the application of a flamelet modeling to investigate the flame behavior, evaporation and behavior of some chemical species in the diesel combustion process in a furnace burner, observing two cases with droplet size injections. many different.

2. DESCRIPTION OF THE MATHEMATICAL MODEL

The solver used for the calculations was CFX v.19.2 © Ansys Europe Ltd based on the finite volume method (Patankar, 1980). The function "power-law" was selected for evaluating the fluxes at the control volume faces and the "up-wind" for interpolation scheme was set. For the pressure-velocity coupling, the SIMPLE algorithm was used and the segregated solution method with implicit linearization was chosen. The discretization scheme applied in this investigation was second-order upwind, which is essential for an accurate modeling of flames although it is very difficult to obtain convergence. The RMS convergence criteria (Root Mean Square) was used and this value was assumed less the 10^{-6} for all variables.

The three-dimensional mathematical model of the combustion chamber is based on time-averaged nonlinear partial differential equations whose general form written in Cartesian tensor notation is

$$\frac{\partial}{\partial t}(\rho\varphi) + \frac{\partial}{\partial x_j}\left(\rho u_j \varphi\right) = S_\varphi + \frac{\partial J_{\varphi,j}}{\partial x_j} \tag{1}$$

where φ is any of Favre averaged transport properties. In a steady-state simulation, as in this case, the transient term may be omitted. The second term on the left represents the advective transport and last term on de right side represents the diffusion of φ. The remaining term S_φ account the sources terms.

The set of equations solved by CFX are mass, momentum, energy and chemical species conservation equations, as well as the equation of state of ideal gas. An Eulerian description for the fluid phase and Lagrangean description for the particle phase (liquid Diesel) was adopted.

Scalar transport equations are solved for velocity, pressure, temperature and chemical species. The bulk motion of the fluid is modeled using single velocity, pressure, temperature, chemical species and turbulence fields (Ansys Inc., 2018).

The standard $k-\varepsilon$ turbulence model was applied to closing the problem due to the averaged Navier-Stokes equations process.

To consider thermal radiation exchanges inside the combustion chamber, the Discrete Transfer Radiation Model (DTRM) is employed (Carvalho et al., 1991), which assumes that the radiation leaving the surface of an element in a given range of solid angles can be approximated by the behavior of a single ray (Ansys Inc., 2018). The effect of the non-gray gaseous mixture was considered by original Gray Gas Model.

2.1 Combustion Modeling

The flamelet concept views the turbulent flame as an ensemble of thin, laminar, locally one-dimensional flamelet structures embedded within the turbulent flow field (Peters, 1984; Peters, 1986; Brain and Peters, 1994).

A common laminar flame type used to represent a flamelet in a turbulent flow is the counterflow diffusion flame. This geometry consists of opposed, axisymmetric fuel and oxidizer jets. As the distance between the jets is decreased and/or the velocity of the jets increased, the flame is strained and increasingly departs from chemical equilibrium until it is eventually extinguished. The species mass fraction and temperature fields can be measured in laminar counterflow diffusion flame experiments, or, most commonly, calculated. For the latter, a self-similar solution exists, and the governing equations can be simplified to one along the axis of the fuel and oxidizer jets, where complex chemistry calculations can be affordably performed.

In the laminar counterflow flame, the mixture fraction, *f*, decreases monotonically from unity at the fuel jet to zero at the oxidizer jet. If the species mass fraction and temperature along the axis are mapped from physical space to mixture fraction space, they can be uniquely described by two parameters: the mixture fraction and the strain rate (or, equivalently, the scalar dissipation, χ, which totally represents the influence of the flow field on the flamelet structure). Hence, the chemistry is reduced and completely described by the two quantities, *f* and χ.

This reduction of the complex chemistry to two variables allows the flamelet calculations to be preprocessed and stored in look-up tables. By preprocessing the chemistry, computational costs are reduced considerably.

The balance equations, solution methods, and sample calculations of the counterflow laminar diffusion flame can be found in several references. Comprehensive reviews and analyses are presented in the works of Bray and Peters (1994), and Dixon-Lewis (1990).

The flamelet approach can be considered as an extension of the "flame sheet" model which assumes infinitely fast chemical reactions. These fast chemistry assumption fails whenever non-equilibrium effects such us extinction, re-ignition, lift-off and blow-out are important. Moreover, these assumption for some intermediate species like CO and H_2 and NOx formation results in an over-prediction of the mass fraction of these species since they are involved in slow reactions. Carbon monoxide (CO) oxidation to carbon dioxide (CO_2) is slow and formation times of thermal nitrogen oxide (NOx) are even longer (Poinsot and Veynante, 2001). This suggests that non-equilibrium effects are important in modelling these flames. The flamelet approach relaxes the infinitely fast chemistry assumption by introducing, in addition

to the mixture fraction, the scalar dissipation rate as a parameter to describe the degree of departure from the equilibrium state (Chou et al., 1998). Some models have been successful in close-to-equilibrium flames (Peters, 1984), nevertheless, far-from-equilibrium effects such as flame extinction are typically present in many flames, and a methodology designed to incorporate these effects is not only desirable but necessary.

However, the *steady flamelet* approach still relies on the assumption that the time scales for chemical kinetics are much shorter than the time scales of convection and diffusion. Under this condition of widely separated time scales, the combustion chemistry reaches a quasi-steady state and immediately adjusts to local flow conditions. Some phenomena, eg radiation heat transfer or pollutant formation of NOx, do not accomplish this requirement of separated time scales. These are slow processes compared to main chemical time scales and can have a characteristic time scale of the same order of magnitude of the convective or diffusive ones.

Therefore, flamelet modeling has the advantage of separating the numerical effort associated with the resolution of small chemical time and length scales from the CFD-computation of the combustion (Bray and Peters, 1994). Concluding from the to eddy dissipation models analogous assumption that the chemical time and length scales are much smaller than the turbulent ones, follows that the flame sheet can merely be stretched and distorted by the smallest turbulent eddies. Therefore, the laminar flame structure is disturbed locally, but preserved.

The flamelet equations are solved in a separate code, interactively coupled with a CFD-code. Each time step the CFD-Code solves its own set of equations, it also makes a call to the flamelet code, which solves the unsteady flamelet equations with time steps that can be much smaller, e.g. during ignition. In this way the time scales of the fluid dynamics and the chemistry are decoupled. The interaction between the CFD-code and the flamelet code is shown schematically in Fig. 1.

The laminar flamelet concept assumption can contribute both in laminar and specially in turbulent flames to reduce this computational effort. Even though this concept is not new, its study and application has increased and improved during the last two decades. Turbulent combustion flames are the main interest and widespread application.

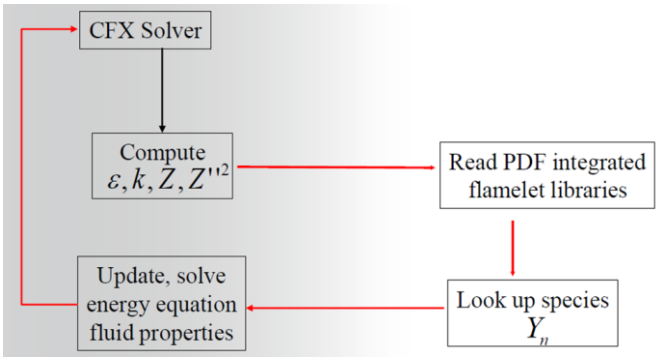

Figure 1. interaction between the CFD-code and the flamelet code.

3. PHYSICAL SYSTEM AND BOUNDARY CONDITIONS

The physical system consists of a burner Doosan Babcock Mark-III of 50MWt installed in a circular combustion chamber for combustion tests with 5 m of the diameter and 11 m of the length, equipped with Y-jet diesel burner. Atomizing fluid is supplied through the central channel and is divided into six jets, one for each individual Y branch. In each "Y," liquid and atomizing fluids strongly interact to generate instabilities in the liquid flow that further cause the breakup into droplets, forming the spray. This nozzle has six exit ports uniformly spaced around the atomizing body. The Fig. 2 shows the burner geometry considered in the study. Fig. 2-c shows the diesel burner detail.

In Tab. 1 are show inlets boundary conditions. The thermal boundary condition of convection was applied to the combustion chamber walls, and it was assumed that heat transfer coefficient is 9.2 W/m²K and internal emissivity is 0.6. The burner walls were modeled as adiabatic with.

Two cases were evaluated in this study with different droplet sizes, Case I with 90 μm drop size and Case II with 50 μm drop size. In both cases, droplets were considered spherical with uniform size.

Table 1. Inlets boundary conditions.

Inlet	Mass flow [kg/s]	Temperature [K]	Swirl
Diesel Fuel	Diesel: 0.24 Air: 0.01	300	0
Core Air	0.5	600	0.9
Primary Air	2.5	600	0
Secondary Air	4.3	600	0.45
Tertiary Air	9	600	0.6

4. MESH

The software Ansys © ICEM CFD was used to compute the geometry and the mesh. Fig. 3 shows the computational mesh composed of approximately 5 million of control volumes. The mesh consists of 2 parts: one in the burner and other in the combustion chamber. In the combustion chamber it is a structured mesh. In the burner it is a hybrid mesh with prismatic elements near the walls and hexagonal elements in the center.

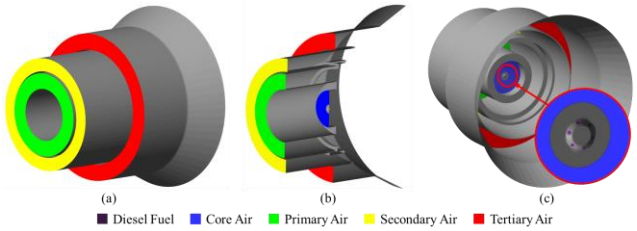

Figure 2. Burner geometry considered in this study. In this figure, colors represent inlets.

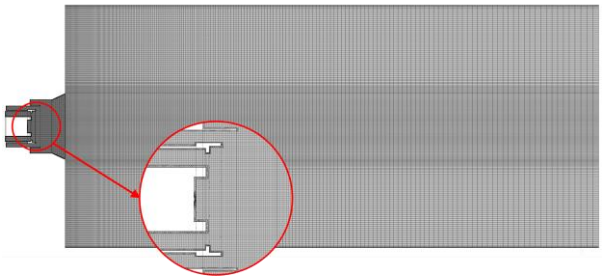

Figure 3. Computational mesh of this study.

5. RESULTS

To analyze the reacting flow structure, the flow is classified into five main zones as shown in Fig. 4: Reverse Zone, External Recirculation Zone, Flame Front, Flame Bulge and Stagnation Zone. As the flow characteristics in the two cases studies are practically identical, was shown only the results for case I. The figure shows that near the fuel injection region the vortices anchor, stabilize the flame and aid shape the spray's spreading angle. In the reverse zone is where the highest temperatures occur, driven by the high concentrations of OH, as will be seen below.

As can be seen in Fig. 5, the stagnation point position occurs when a zero axial velocity isoline (red line) sticks to the wall, part of the oxygen continues its way toward the exit, but part circulates and returns, creating a recirculation zone with negative velocity component. The center of this recirculation vortex is determined by the intersection of axial and radial zero velocity isolines (blue line), that is, the existence of a region with zero axial and radial velocity causes a vortex to be created and thus a recirculation zone.

The reverse zone is delimited by a zero axial velocity isoline, as shown in Fig. 5. Recirculation in this zone generates a suction effect forming a flame front protuberance, called the Flame Bulge, which stabilizes the intermediate flame zone. In this zone there is a drastic increase in the OH mass fraction, as will be seen below. The most important effect of this recirculation zone is to configure the shape of the flame.

Although, the Aerodynamically Air Staged Burner used in the present study is specially configured for proper mixing of the flow, flow condition is also responsible for the generation of recirculation regions inside the furnace.

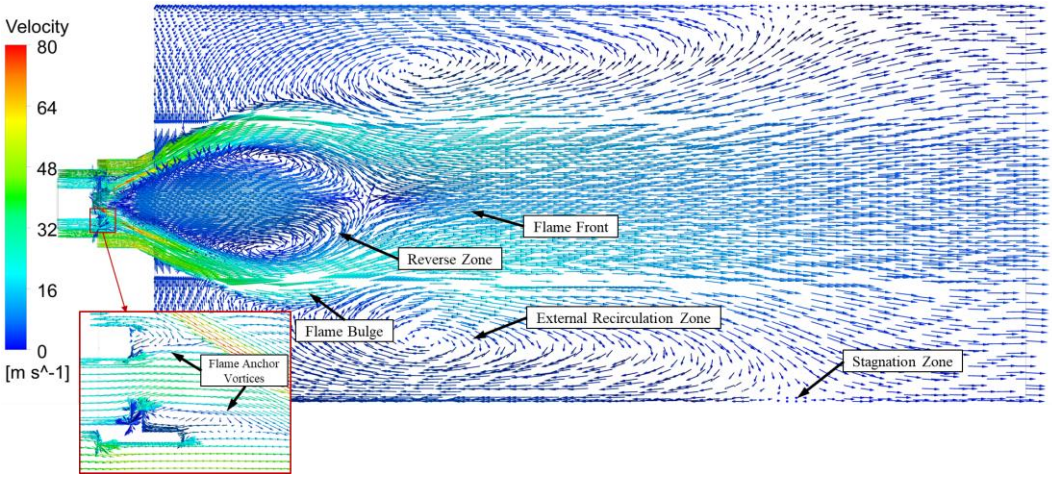

Figure 4. Velocity vectors in a central vertical plane in the combustion chamber, colored by velocity distribution for the Case I.

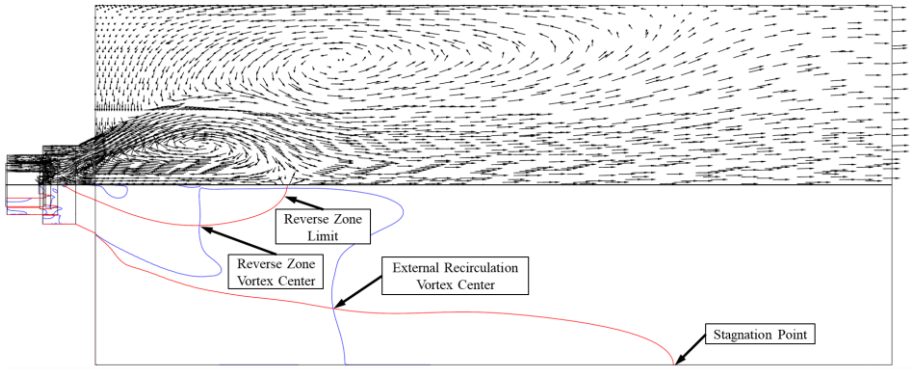

Figure 5. Flow vectors and isolines (red line is zero axial velocity and blue line is zero radial velocity) in a central vertical plane in the combustion chamber for the Case I.

In order to visualize the overall flame temperature, its distributions on the vertical plane axially along the center of the furnace are presented in Fig. 6. It is observed from the figure that the flame starts at the burner exit as expected and extended further approximately 2.0 m in the axial direction in two cases. In the figure, it can be noted that the higher temperatures of both cases are concentrated in the Reverse Zone, and Case II developed a larger high temperature region with this region closer to the burner outlet and further of the flame front, than Case I.

Figure 7 describes the axial distributions of OH mass fraction in the same plane. The behavior is similar to temperature, where the highest OH concentrations are located in the Reverse Zone Vortex Center (Fig. 5). As can be seen, the highest concentrations are found in Case II, which justifies the high temperature region observed in Fig. 6.

Figure 8 describes the axial distributions of O_2 mass fraction. It is noted that Case II consumes oxygen earlier which indicates higher fuel oxidation rates near the injector.

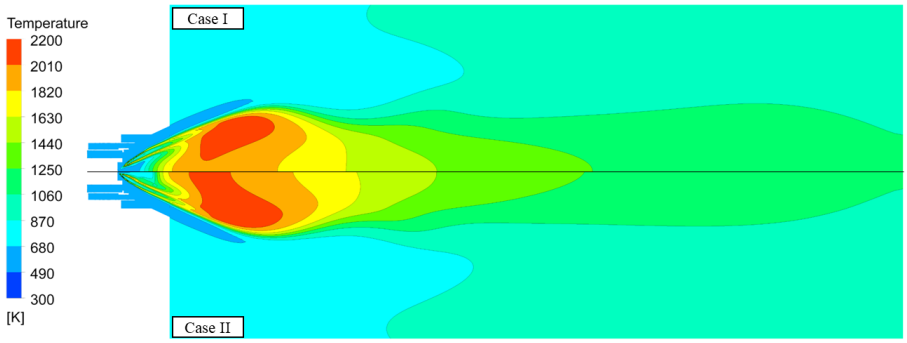

Figure 6. Temperature distribution in central plane for the Case I (top) and Case II (bottom).

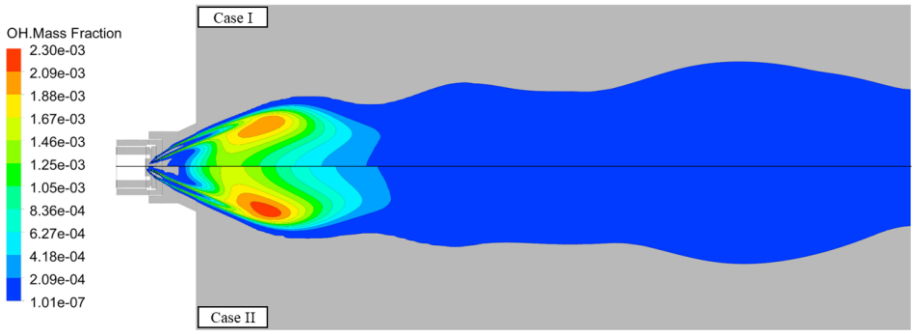

Figure 7. OH mass fraction distribution in central plane for the Case I (top) and Case II (bottom).

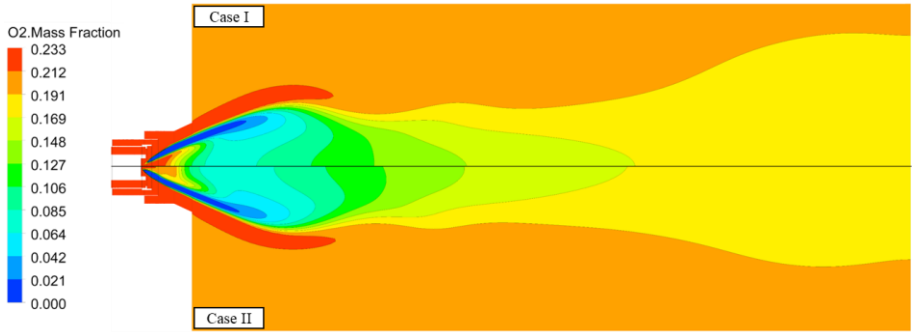

Figure 8. O_2 mass fraction distribution in central plane for the Case I (top) and Case II (bottom).

Figure 9 represents the temperature and diameter behavior of a drop along a particle track for both cases studied. As expected, Case II (smaller drop) gained temperature faster, with a warming rate almost 2 times higher than Case I. It can also be observed that Case I took a distance of 0.67 m to evaporate by while in Case II it took 0.41 m, because of this, the energy absorbed by the droplet in Case I was higher, resulting in a higher droplet temperature than in Case II. This is also since, in case I, the droplets traveled longer paths and entered higher temperature regions within the combustion chamber.

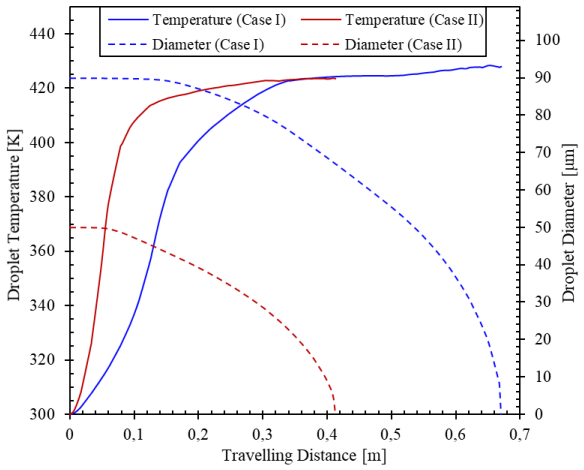

Figure 9. Temperature and droplet diameter behavior away from a particle track for both cases.

Figures 10 and 11 show the behavioral graphs of CO, O2, Diesel Steam and Droplet Temperature along the droplet tracking. Through the analysis of the graphs it is observed that large drops (Case I) take longer to evaporate, following a larger path, behavior also observed in Fig. 9. The high evaporation rates of diesel in Case II are due to the larger effective surface area of the droplets in contact with the environment, which is due to the fact that smaller droplet sizes lead to a larger number of droplets to maintain the same fuel mass flow rate, thus increasing the total surface area of the drops. CO production in Case II begins closer to the injector due to higher fuel droplet oxidation rates.

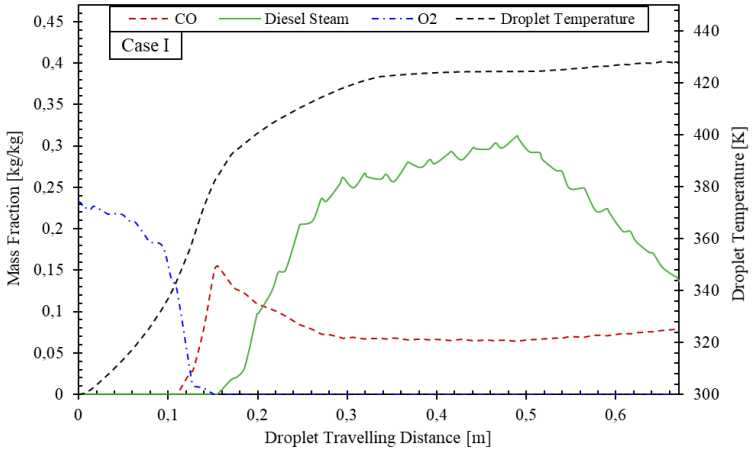

Figure 10. Mass fractions and temperature behavior away from a particle track for the Case I.

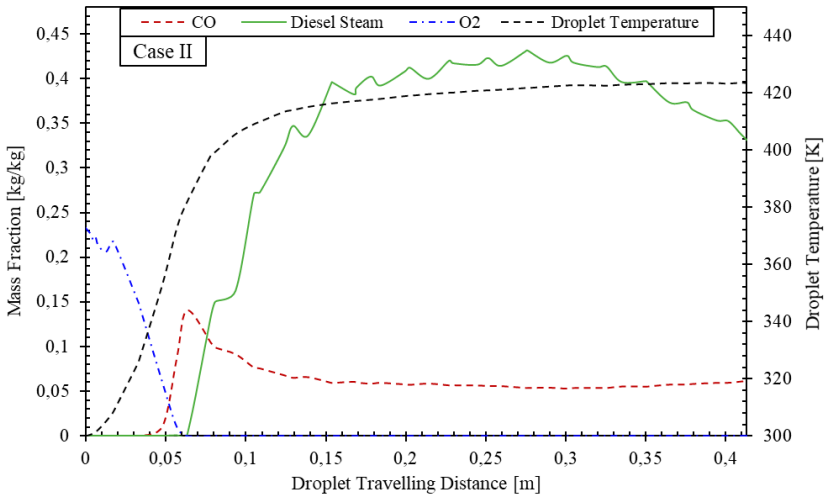

Figure 11. Mass fractions and temperature behavior away from a particle track for the Case II.

6. CONCLUSION

Because larger droplets have greater mass, they will require more energy than smaller droplets to reach the same temperatures and evaporate. Thus, large drops take longer to evaporate, absorbing more energy from the flame, diluting it, and consequently producing less intense flame.

In addition, the total surface area of a spray with smaller droplets also plays a key role in fuel evaporation and oxidation, because, with greater area, evaporation rates increase allowing the fuel to evaporate absorbing less flame energy, so the oxidation of the fuel also begins closer to the injector, which contributes to a more intense flame being produced.

7. ACKNOWLEDGEMENTS

We acknowledge Energy of Portugal EDP for the financial and technical support to this project; Vanz acknowledges CNPq for his MSc grant; Smith Schneider acknowledges CNPq for his research grant (PQ305357/2013-1).

8. REFERENCES

Ansys Inc., 2018 “User's guide – CFX”. Solver Theory.

Bray, K.N.C and Peters, N., 1994. “Laminar Flamelets in Turbulent Flames”, In *Turbulent Reacting Flows*, Libby, P.A. and Williams, F.A. Eds, Academic Press, London.

Carvalho, M. G.; Farias, T. and Fontes, P., 1991. “Predicting Radiative Heat Transfer in Absorbing, Emitting and Scattering Media Using the Discrete Transfer Method”. ASME HTD, Vol. 160, pp. 17–26.

Dixon-Lewis, G., 1990. "Structure of Laminar Flames". In *23rd Symp. (Int'l.) on Combustion*. The Combustion Institute. pp. 305–324.

Dorigon, L.J., Duciak, G., Brittes, R., Cassol, F., Galarça, M., França, F.H.R., 2013. “WSGG correlations based on HITEMP 2010 for computation of thermal radiation in non-isothermal, non-homogeneous H2O/CO2 mixtures”, *International Journal of Heat and Mass Transfer*, Vol. 64, pp. 863–873.

Hottel, H.C. and Sarofim, A.F., 1967. “Radiative Transfer”. New York, McGraw-Hill Book Company.

Patankar, S.V., 1980. “Numerical Heat Transfer and Fluid Flow, Hemisphere”, New York.

Peters, N., 1984. “Laminar diffusion flamelet models in non-premixed turbulent combustion”. *Progress in Energy and Combustion Science*, Vol. 10, pp. 319–339.

Peters, N., 1986. “Laminar flamelet concepts in turbulent combustion”. In *Proceedings of the Twenty-First Symposium (International) on Combustion*, pp. 1231–1250.

Poinsot, T. and Veynante, D., 2001. *Theorical and Numerical Combustion*. R.T. Edwards, Inc.

Chou, C.P., Chen, J.Y., Yam, C.G. and Marx, K.D., 1998. “Numerical modeling of NO formation in laminar Busen flames – A flamelet approach”. *Combustion and Flame*, Vol. 114, pp. 420–435.

9. RESPONSIBILITY NOTICE

The authors are the only responsible for the printed material included in this paper.